then measured using an 8410B HP network analyzer. As we expected, the measured reflection coefficient was not zero (i.e., the value of the characteristic impedance of the manufactured line is not 50 Ω, as we desire). This, of course, is due to the effect of manufacturing tolerances. The top cover was then moved up and down until matching was obtained.

It may be pointed out that it is not easy, in practice, as it seems from this example, to compensate for the effect of manufacturing tolerances because, in practice, actual circuits contain more than one line, each having different manufacturing tolerances.

Example 2

The bandpass parallel-coupled filter of [3], and shown in Fig. 3, is redesigned for the same specifications, but the response is optimized for a shield height ratio $h_1/h_2 = 2$ using the state-space method of [5]. The new circuit dimensions are given in Table I. Both the computed and measured responses, with and without the top cover, are shown in Fig. 4. Measured and calculated responses show that, in shielded microstrip circuits, the response may be controlled by varying the position of the top cover. It may be pointed out that the theoretical response, with the presence of the top cover, is calculated at a shield heights ratio $h_1/h_2 = 2$. While the measured response, with the presence of the top cover, is obtained by moving the top cover up and down until we obtain a response that meets our desired specifications (i.e., not necessarily at shield heights ratio $h_1/h_2 = 2$).

From the foregoing examples, we suggest a shielded microstrip circuit with a variable shield heights ratio that can be used for a mechanical tuning of a given shielded microstrip circuit.

Special substrate holders (fixtures) with variable shield heights ratios have been manufactured for use during the above-mentioned measurements.

IV. Conclusion

It should be pointed out that the shielded microstrip circuit with a variable shield heights ratio will not perform magic. It is not expected to be able to compensate for any and all possible manufacturing tolerance combinations. However, an experienced designer can make use of this construction to improve the performance of his designed circuit. It also should be pointed out that we do not call for production of shielded microstrip circuits with variable shield heights ratios for normal usage. We only call for manufacturing circuits with variable shield heights ratios during the prototype stage of testing the designed circuit. The position of the top cover is then varied until the response of the prototype meets the desired specifications. Then the final circuits should be manufactured according to the prototype.

References

[1] R. Garg, "The effect of tolerances on microstripline and slotline performance," *IEEE Trans. Microwave Theory Tech.*, vol. MTT-26, pp. 16–19, Jan. 1978.

[2] S. D. Shamasundara and K. C. Gupta, "Sensitivity analysis of coupled microstrip directional coupler," *IEEE Trans. Microwave Theory Tech.*, vol. MTT-26, pp. 788–794, Oct. 1978.

[3] S. S. Bedair and M. I. Sobhy, "Accurate formulas for computer-aided design of shielded microstrip circuits," *Proc. Inst. Elec. Eng.*, vol. 127, pt. H., pp. 305–308, Dec. 1980.

[4] S. L. March, "Microstrip packaging: Watch the last step," *Microwaves*, vol. 20, pp. 83–94, Dec. 1981.

[5] M. I. Sobhy, S. S. Bedair, and M. H. Keriakos, "State-space approach for the analysis of networks containing lossy coupled transmission lines in inhomogeneous media," *Proc. Inst. Elec. Eng.*, vol. 128, pt. G., pp. 89–95, June 1982.

Heating Pattern in a Multi-layered Material Exposed to Microwaves

M. NACHMAN, SENIOR MEMBER, IEEE, AND G. TURGEON

***Abstract*—The electromagnetic-induced heating pattern in a multi-layered slab material exposed to uniform plane microwaves is studied. A general expression taking into account the multiple reflections at the interfaces is derived for the power dissipated per unit volume in the medium. A numerical method is developed for solving the heat transport equation describing the temperature distribution in this material. A steady, as well as a transient solution is obtained for either a Dirichlet- or a Neumann-type of boundary condition. The effect on the temperature distribution of a cooling fluid circulating inside the slab is considered.**

The method is applied to the special case of a three-layered material having characteristics similar to those of a biological structure. The possibility of achieving a preferential heating of one of the layers by means of standing waves created with the aid of a flat reflector is demonstrated.

I. Introduction

The electromagnetic-induced heating pattern in a slab material exposed to a uniform plane microwave may be obtained from the one-dimensional heat transport equation (HTE). In the presence of a circulating cooling fluid in the material this equation is [1]

$$\rho_m c \frac{\partial T}{\partial t} = k_t \frac{\partial^2 T}{\partial x^2} - Vs(T - T_0) + Q(x,t) \qquad (1)$$

where

ρ_m = material density,
c = specific heat,
k_t = thermal conductivity,
Vs = product of flow and heat capacity of the cooling fluid,
T = material temperature,
T_0 = temperature of the fluid entering the material, and
$Q(x,t)$ = electromagnetic power dissipated per unit volume.

An analytical steady-state solution of this equation can be found in [2] for the case of a single finite or semi-infinite layer. Foster, Kritikos, and Schwan [1] obtained a transient solution for a semi-infinite single-plane layer and applied it for determining the temperature distribution in living tissues exposed to microwave radiation. In their equation, the term $Vs(T - T_0)$ represented the contribution of the blood convection to the heat dissipation in the tissue.[1]

More recent attempts to solve the steady-state heat-transport equation by numerical methods are described in [4] and [5]. Numerical calculations of energy deposition and temperature distribution in biological tissues exposed to plane electromagnetic waves are reported in [6] and [7].

In what follows, a numerical method for solving the transient heat transport equation in a multi-layered material, with either a Dirichlet- or a Neumann-type of boundary condition, is presented. The cooling effect due to a fluid circulating through the

Manuscript received July 12, 1983; revised January 19, 1984.

The authors are with the Ecole Polytechnique of Montreal, Electrical Engineering Dept., P.O. Box 6079, Station "A", Montreal, Quebec, Canada H3C 3A7.

[1] A more correct approach to evaluating this contribution was proposed by Wulff [3].

0018-9480/84/0500-0547$01.00 ©1984 IEEE

material is taken into account. At the same time, the possibility of achieving a preferential heating of one of the layers, by means of standing waves created with the aid of a flat reflector, is demonstrated. The method is applied to the special case of a three-layered material, having characteristics similar to those of a biological structure.

II. Power Input Due to the Presence of a Microwave Field

For a time-harmonic electromagnetic (EM) field of angular frequency ω, the term $Q(x,t)$ accounting for the heat input due to the microwaves is given by

$$Q(x,t) = P = \frac{\omega \epsilon'' |\bar{E}|^2}{2} \tag{2}$$

where ϵ'' is the imaginary part of the complex permittivity and $\bar{E}$ the electric field.

In a multi-layered slab, material exposed, at normal incidence, to a plane, linearly polarized microwave (Fig. 1), the electric field in the kth layer is given by [8], [9]

$$\bar{E}_k = E_{io}\left(\tau_k e^{-\gamma_k x} + \rho_k e^{\gamma_k x}\right)\hat{y} \tag{3}$$

where

E_{io} = amplitude of the incident electric field,
γ_k = propagation constant of layer k,
τ_k = total transmission coefficient of layer k, and
ρ_k = total reflection coefficient of layer k.

Let $(n-2)$ be the number of layers in a slab placed in air. Then the system consisting of the slab and the two adjoining air layers of infinite extent A_1 and A_n may be considered as an n-layered structure. The boundary conditions for the tangential components of the electric and magnetic fields at the $(n-1)$ interfaces of this structure represent a set of $2(n-1)$ linear equations for the $2n$ unknown quantities ρ_k and τ_k. The transmission coefficient in the first layer (A_1) is $\tau_1 = 1$ and the reflection coefficient in the nth layer (A_n) is zero.[2] We are thus left with $(2n-2)$ unknown quantities τ_k, ρ_k, which may be obtained by solving the set of $2(n-1)$ equations[3].

Once τ_k and ρ_k are known, the magnitude of the electric field may be computed from (3). For simplicity sake, the index k has been dropped in what follows. We have

$$|E| = |E_{io}\tau e^{-\gamma x}|\left|1 + \frac{\rho}{\tau} e^{2\gamma x}\right|. \tag{4}$$

Since γ, τ, and ρ are, generally speaking, complex quantities, we have

$$\gamma = \alpha + j\beta$$
$$\tau = |\tau| \angle \varphi$$
$$\rho = |\rho| \angle \theta .$$

The expression $|1 + \rho/\tau e^{2\gamma x}|$ in (4) may now be written as

$$\left|1 + \frac{\rho}{\tau} e^{2\gamma x}\right| = |1 + e^{2\alpha x}[A\cos 2\beta x - C\sin 2\beta x + j(C\cos 2\beta x + A\sin 2\beta x)]|$$

[2]If a perfect flat reflector is placed in the air at a certain distance from the slab (see Fig. 1), then $\rho_n = -\tau_n$.

[3]In the general case, τ_k and ρ_k may be complex quantities.

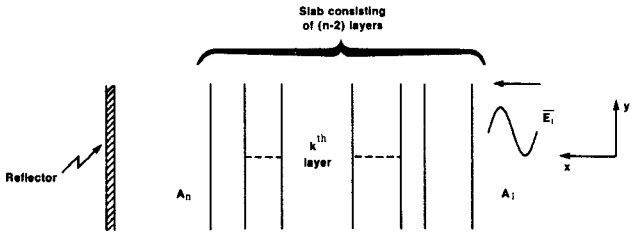

Fig. 1. Geometry of the multi-layered structure.

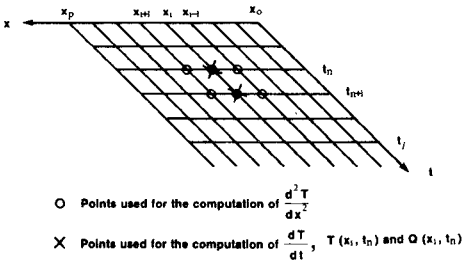

Fig. 2. Grid used in the numerical method.

where

$$A = \frac{|\rho|}{|\tau|}\cos(\theta - \varphi)$$
$$C = \frac{|\rho|}{|\tau|}\sin(\theta - \varphi). \tag{5}$$

Taking into account (4), the expression for P becomes

$$P = \frac{\omega \epsilon''}{2}|E_{io}|^2\left[|\tau|^2 e^{-2\alpha x} + |\rho|^2 e^{2\alpha x} + 2|\rho||\tau|\cos(2\beta x + \theta - \varphi)\right]. \tag{6}$$

For a time-harmonic EM field, P is constant in time. However, depending on the characteristics of the signal provided by the microwave source, P may exhibit a variation in time, which has to be taken into account in solving the HTE.

III. Numerical Solution of the HTE for a Single Homogeneous Slab

We will now describe the numerical method used for solving the HTE. We will apply it first to the HTE in a single homogeneous slab. Subsequently, we will generalize the results for the case of a multilayered material, each layer being homogeneous and having certain given electrical and thermal properties.

For a single-plane, homogeneous layer, the HTE (1) may be written as

$$\frac{dT(x,t)}{dt} = \eta \frac{d^2T(x,t)}{dx^2} - \zeta[T(x,t) - T_0] + \kappa Q(x,t) \tag{7}$$

where

$$\eta = \frac{k}{\rho_m c} \quad \zeta = \frac{Vs}{\rho_m c} \quad \kappa = \frac{1}{\rho_m c}.$$

Discretization of the continuous problem is accomplished by substituting the differentials by finite differences.

For this purpose, a network of equally spaced grid points (x_i, t_n) is established in the (x,t) plane (Fig. 2). The time

derivative of T may now be expressed as

$$\frac{dT}{dt} \simeq \frac{T_i^{n+1} - T_i^n}{\Delta t}$$

where $T_i^n = T(x_i, t_n)$ and $\Delta t = t_{n+1} - t_n$.

An approximate expression for the space derivative may be obtained by applying the weighted implicit method [10]. It is known that implicit numerical methods provide a better approximation than explicit methods to the solution of partial differential equation describing transport phenomena. We have

$$\frac{d^2T}{dx^2} \simeq \nu \left.\frac{d^2T}{dx^2}\right|^{n+1} + (1-\nu) \left.\frac{d^2T}{dx^2}\right|^{n} \tag{8}$$

where

$$\nu = \text{weighting factor} \qquad (0 < \nu < 1)^4$$

$$\left.\frac{d^2T}{dx^2}\right|^{n+1} \simeq \frac{T_{i+1}^{n+1} - 2T_i^{n+1} + T_{i-1}^{n+1}}{\Delta x^2}$$

$$\left.\frac{d^2T}{dx^2}\right|^{n} \simeq \frac{T_{i+1}^{n} - 2T_i^{n} + T_{i-1}^{n}}{\Delta x^2}$$

where

$$\Delta x = x_{i+1} - x_i.$$

We also have

$$T(x_i, t_n) = T_i^n = \nu T_i^{n+1} + (1-\nu) T_i^n \tag{9}$$

and

$$Q(x_i, t_n) = \nu Q_i^{n+1} + (1-\nu) Q_i^n. \tag{10}$$

The grid points considered for the computation of (8), (9), and (10) are shown in Fig. 2. With (8), (9), and (10), the HTE (1) becomes

$$\begin{aligned}\frac{T_i^{n+1} - T_i^n}{\Delta t} = \eta \Bigg[& \nu \frac{T_{i+1}^{n+1} - 2T_i^{n+1} + T_{i-1}^{n+1}}{\Delta x^2} \\ & + (1-\nu) \frac{T_{i+1}^{n} - 2T_i^{n} + T_{i-1}^{n}}{\Delta x^2} \Bigg] \\ & - \zeta \left[\nu T_i^{n+1} + (1-\nu) T_i^n - T_0 \right] \\ & + \kappa \left[\nu Q_i^{n+1} + (1-\nu) Q_i^n \right]. \end{aligned} \tag{11}$$

Rearranging the terms in (11) yields

$$\begin{aligned} & -\lambda \nu T_{i-1}^{n+1} + (1 + 2\lambda\nu + \zeta \nu \Delta t) T_i^{n+1} - \lambda \nu T_{i+1}^{n+1} \\ & \quad = \lambda (1-\nu) T_{i-1}^n + [1 - \zeta \Delta t (1-\nu) - 2\lambda (1-\nu)] T_i^n \\ & \qquad + \lambda (1-\nu) T_{i+1}^n + \zeta \Delta t T_0 + \kappa \Delta t \left[\nu Q_i^{n+1} + (1-\nu) Q_i^n \right] \end{aligned} \tag{12}$$

where

$$\lambda = \frac{\eta \Delta t}{(\Delta x)^2}.$$

For each t_n, we now have a set of $(p-1)$ equations which, combined with the two boundary conditions (at $i = 0$ and $i = p$), make it possible to derive the $p+1$ values T_i^{n+1} as functions of T_i^n. Once the initial temperatures T_i^o are known, the final temperature distribution in the slab may be computed.

[4] If $\nu = \frac{1}{2}$, it is known as the Crank-Nicholson factor.

IV. Boundary Conditions

The boundary conditions may be of either the Neumann or the Dirichlet type.

In the first case, the temperature gradient at the slab boundary is given. We will consider here the simpler case

$$\frac{dT}{dx} = C$$

where C is a fixed constant. We have now for the two boundaries

$$T_0^{n+1} = T_1^{n+1} - C_1 \Delta x \qquad \text{at } x = x_0$$

and

$$T_p^{n+1} = T_{p-1}^{n+1} - C_2 \Delta x \qquad \text{at } x = x_p.$$

In the case of a Dirichlet type of boundary condition, the temperature at the two slab boundaries are known

$$T_0^{n+1} = C_2 \quad \text{and} \quad T_p^{n+1} = C_4$$

where C_3 and C_4 are given constants. The set of equations (12) may be solved with either one of these conditions and the temperature in the grid points at a certain moment t_n may be computed. Subsequently, the temperature distribution at $t_n + \Delta t$ may be derived by solving the same set of equations (12), with the temperature distribution at t_n as the new initial condition. The transient solution may thus be obtained for any t_n. The intervals Δt and Δx have to be small enough in order to achieve a satisfactory degree of precision. The solution is unconditionally stable for $\Delta t > 0$ if $\nu > 0$.

V. Numerical Solution of the HTE for a Multi-Layered Material

The numerical method developed for a single layer may easily be generalized for the case of a multi-layered material, each layer being characterized by the set of parameters η, ζ, κ. The procedure consists of adopting for these parameters the set of values corresponding to the current layer as soon as the solution point crosses the boundary between the previous layer and the current one. It is therefore unnecessary to write explicitly the boundary conditions at each of the interfaces between adjoining layers in order to solve the problem. The only boundary conditions required are those at the two interfaces between the multilayered structure and the surrounding medium.

VI. Three-Layered Material

The numerical method described above has been applied to the special case of a semi-infinite three-layered slab material exposed to a uniform plane microwave. The temperature distribution has been computed for the following situations:

a) thermally insulated structure with zero fluid flow;

b) structure cooled by a circulating fluid.

In both cases, the effect on the temperature distribution of a flat reflector located outside the structure has been analyzed.

A. Thermally Insulated Three-Layered Material.

The temperature distribution has been computed for a structure identical to that considered by De Wagter *et al.* [4] (see Fig. 3). The structure is thermally insulated with respect to the surrounding medium and no cooling fluid circulates inside it. Since there is no heat loss either to a cooling fluid or at the slab surface, the temperature inside the material will exhibit a steady

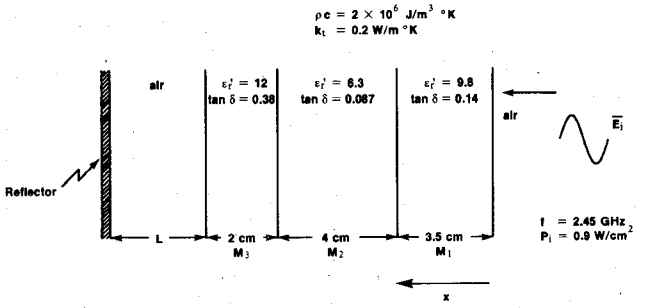

Fig. 3. Physical properties of the three-layered system.

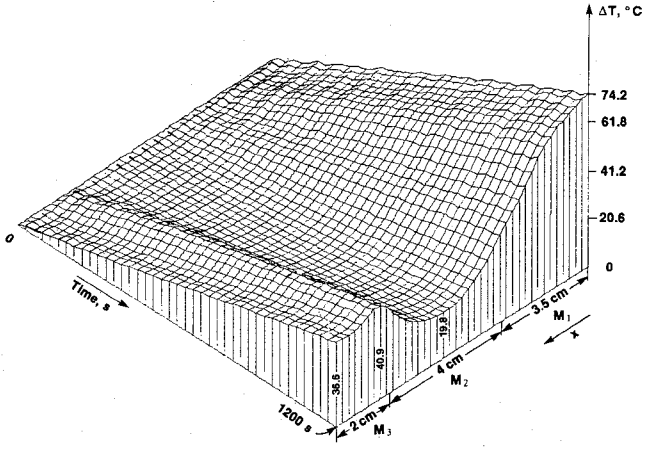

Fig. 4. Evolution in time of the temperature profile in a thermally insulated three-layered material.

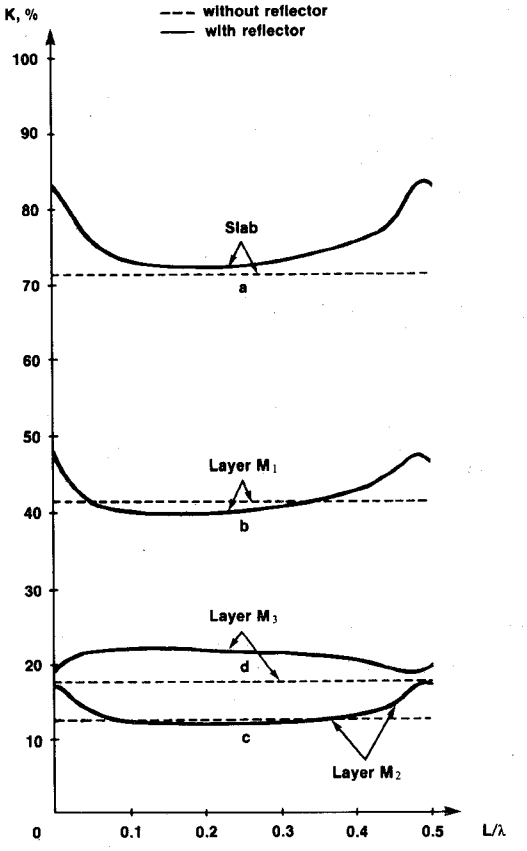

Fig. 5. Heating efficiency in a three-layered material in the absence (dashed line) and in the presence (full line) of a reflector.

rise. The evolution in time of the temperature profile for such a structure is plotted in Fig. 4 for a frequency $f = 2.45$ GHz of the microwaves and an incident power per unit area $P_i = 0.9$ W/cm^2. The results obtained with the method described here are in excellent agreement with those found by De Wagter *et al.* [4] by a different method, under identical physical conditions.

The effect on the temperature distribution of the waves reflected by a reflector placed at a certain distance L from the boundary of the structure (Fig. 3) may be inferred from the plots in Fig. 5. Here the heating efficiency K[5] is represented as a function of L (expressed in free-space wavelengths), for the slab as a whole (curve a) as well as for each of the three layers (curves b, c, d). It is seen that the highest yield is achieved for $L = 0.49\lambda$ and the lowest for $L = 0.2\lambda$. The temperature profile for these two extreme cases are plotted, respectively, in Figs. 6[6] (maximum yield) and 7 (minimum yield). It is seen that a significant change in the temperature profile in the three-layered structure occurs due to the presence of the reflector. A noticeable rise in temperature takes place especially in the third layer (22.7 percent), as well as in the first layer close to the boundary with the surrounding medium. At this boundary, a temperature increase of about 20 percent occurs in the first 20 min after the start of the irradiation process.

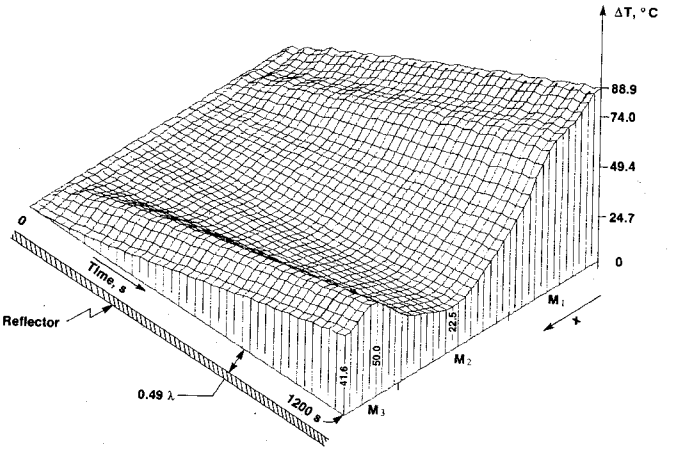

Fig. 6. Evolution in time of the temperature profile in a thermally insulated three-layered material in the presence of a reflector ($L = 0.49\lambda$).

[5]The heating efficiency in a layer bounded by the planes x_a and x_b is given by

$$K = \frac{\int_{x_a}^{x_b} Q(x,t)\,dx}{P_i}.$$

The quantity K is proportional to the specific absorption rate (SAR) in the material.

[6]Note that the temperature scales are different in Figs. 4, 6, 7, 8, 9.

B. Three-Layered Material Cooled by a Circulating Fluid.

The effect of a fluid circulating through one of the layers will now be analyzed. We consider here $Vs = 0.0078$ J/cm^3/s °K in layer 1 and zero in the other two layers. This value of Vs corresponds to that employed by Schwan and Kritikos [11] for describing the heat dissipation by blood in living tissues. We will also consider that at x_0 (Fig. 2) the temperature is maintained constant during exposure to microwaves, whereas at x_p the material is thermally insulated ($dT/dx = 0$). The evolution in time of the temperature profile is plotted in Fig. 8 in the absence and in Fig. 9 in the presence of a reflecting surface (at $L = 0.49\lambda$).

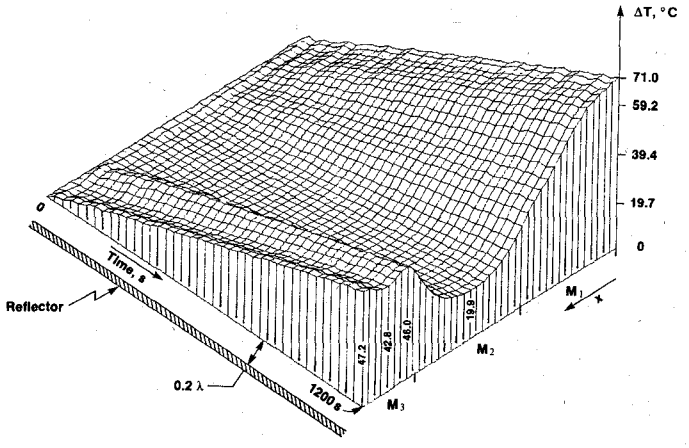

Fig. 7. Evolution in time of the temperature profile in a thermally insulated three-layered material in the presence of a reflector ($L = 0.2\lambda$).

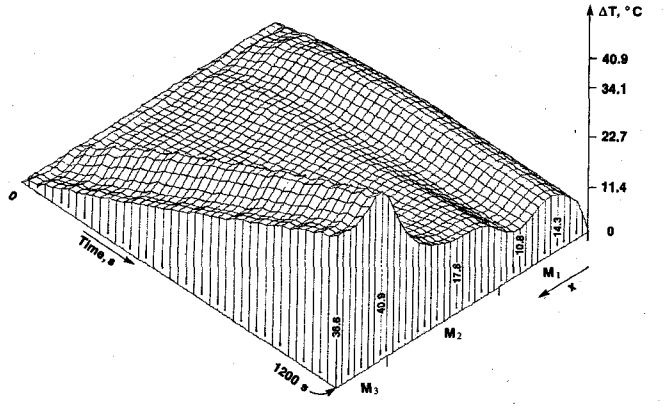

Fig. 8. Evolution in time of the temperature profile in a slab, thermally insulated at x_p, with a constant temperature maintained at x_o and with refrigeration in the M_1 layer ($Vs = 0.0078$ J/cm/s °K).

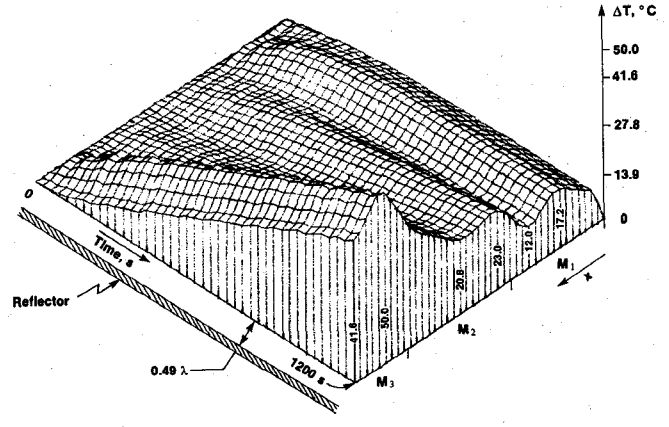

Fig. 9. Evolution in time of the temperature profile in a slab, thermally insulated at x_p, with a constant temperature maintained at x_o and with refrigeration in the M_1 layer ($Vs = 0.0078$ J/cm^3/s °K), in the presence of a reflector at $L = 0.49\lambda$.

By comparing the plots of Figs. 4 and 8, it is readily seen that even a relatively mild cooling due to the circulating fluid greatly alters the heating pattern in the material (Figs. 8 and 9). As was to be expected, the cooling fluid is effective in limiting the temperature rise of the material. The effect is, of course, very pronounced in the layer M1 through which the fluid is circulating, as well as in the adjoining region of the M2 layer. A steady-state temperature is reached very soon (8 min) after the beginning of the irradiation process. However, in layer M3 the temperature rises steadily during the first 20 min and the maximum reached is approximately the same as in the absence of the circulating fluid. It is also important to notice the effectiveness of the reflector in changing the heating pattern in the material. A preferential heating of layer M3 is accomplished in the structure, the temperature in this layer being increased by nearly 24 percent.

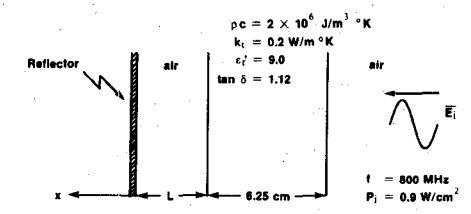

Fig. 10. Physical properties of the slab used for the analysis of the heating pattern in the presence of a reflector.

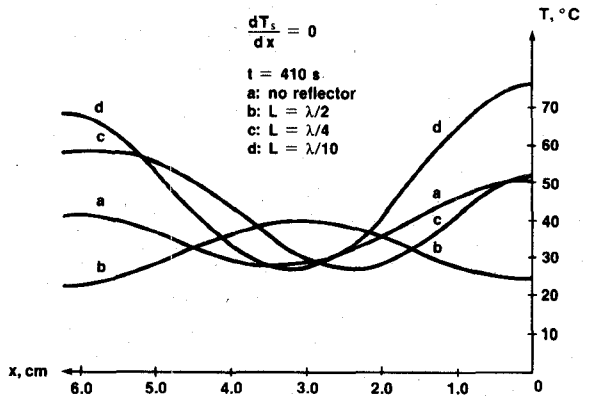

Fig. 11. Temperature profile in a homogeneous slab in the absence (curve a) and in the presence of a reflector (curves b, c, d). Boundary condition: $dT_s/dx = 0$. Irradiation time: 410 s.

At this point we would like to stress the fact that the usefulness of a reflector in changing the heating pattern has been demonstrated here for the simple case of a material consisting of several plane layers. In order to assess the possible application of this technique to the preferential heating of certain regions in the human body, the temperature pattern in models involving more complicated geometries, simulating the irregular shapes of human organs or of tumors, should first be analyzed (see, for instance, [6]).

VII. Preferential Heating in a Homogeneous Slab Material

The possibility of achieving a preferential heating of a certain region of a slab material, by means of standing waves created with the aid of a flat reflecting surface placed outside the material, will now be analyzed in more detail for the simpler case of a homogeneous slab material having the properties as indicated in Fig. 10. In Figs. 11 and 12, the temperature profile in the material exposed to microwaves ($f = 800$ MHz) transporting 0.9 W/cm^2 is represented in the absence (curve $\underline{a}$) and in the presence of the reflector (curves $\underline{b}, \underline{c}, \underline{d}$). In Fig. 11, the material is insulated from the surrounding medium ($dT/dx = 0$), whereas in Fig. 12 the temperatures at the two boundaries are maintained at the initial temperature of 20 °C. In both cases, the profile has been com-

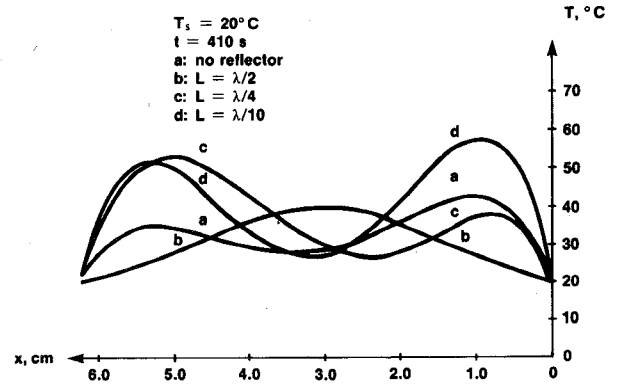

Fig. 12. Temperature profile in a homogeneous slab in the absence (curve *a*) and in the presence of a reflector (curves *b*, *c*, *d*). Boundary conditions: $T_s = 20.0$ °C. Irradiation time: 410 s.

puted at $t = 410$ s after the beginning of the heating process. It is evident that a preferential heating by the microwaves of a certain region in the material may be achieved by adequately selecting the distance between the reflector and the slab boundary.

References

[1] K. R. Foster, H. N. Kritikos, and H. P. Schwan, "Effect of surface cooling and blood flow on the microwave heating of tissue," *IEEE Trans. Biomed. Eng.*, vol. BME-25, p. 313, 1978.
[2] L. C. Thomas, *Fundamental of Heat Transfer*. Englewood Cliffs, NJ: Prentice-Hall, 1980.
[3] W. Wulff, "The energy conservation equation for living tissue," *IEEE Trans. Biomed. Eng.*, vol. BME-21, p. 494, 1974.
[4] C. De Wagter, M. De Pourca, and W. Van Loock, "Microwave heating of laminated materials," in *Dig. Microwave Power Symp.* (Toronto), 1981, p. 225.
[5] L. Krul, E. Attema, and C. de Haan, "Modelling of microwave heating processes," in *Dig. Microwave Symp.* (Ottawa), 1978, p. 77.
[6] R. Zimmer and C. M. Gros, "Numerical calculation of electromagnetic energy and temperature distribution in a microwave irradiated breast carcinoma. Preliminary results," *J. Microwave Power*, vol. 14, p. 155, 1979.
[7] M. van Sliedregt, "Computer calculations of a one-dimensional model, useful in the application of hyperthermia," *Microwave J.*, vol. 26, p. 113, 1983.
[8] G. Turgeon, "Etude de la distribution de la puissance dans un corps stratifié en présence d'une onde électromagnétique stationnaire", Final Projet Rep., Ecole Polytechnique of Montreal, 1981.
[9] G. Turgeon and M. Nachman, "Puissance dissipée par des microondes se propageant dans un milieu stratifié," in *Annales des Communications ACFAS 1981*, 49e Congrès, vol. 48, 1981, p. 95.
[10] B. Carnahan, H. A. Luther, and J. O. Wilkes, *Applied Numerical Methods*. New York: Wiley, 1969, pp. 443–464.
[11] H. N. Kritikos and H. P. Schwan, "Potential temperature rise induced by electromagnetic field in brain tissues," *IEEE Trans. Biomed. Eng.*, vol. BME-26, p. 29, 1979.

On Temperature Characteristics for a GaAs Monolithic Broad-Band Amplifier Having Resistive Loads

KAZUHIKO HONJO, MEMBER, IEEE

Abstract—**Temperature characteristics for a GaAs monolithic broad-band amplifier having resistive loads were investigated. It was demonstrated that gain versus temperature characteristics for the amplifier are self-compensated and that the bandwidth for the amplifier becomes narrow when ambient temperature increases.**

Manuscript received August 24, 1983; revised January 16, 1984.
The author is with Microelectronics Research Laboratories, NEC Corporation, 1-1, Miyazaki, 4-chome, Miyamae-ku, Kawasaki, Kanagawa, 213, Japan.

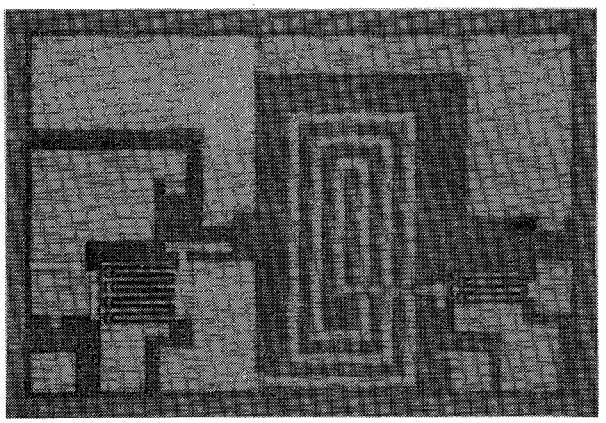

Fig. 1. Chip photograph for GaAs monolithic broad-band amplifier.

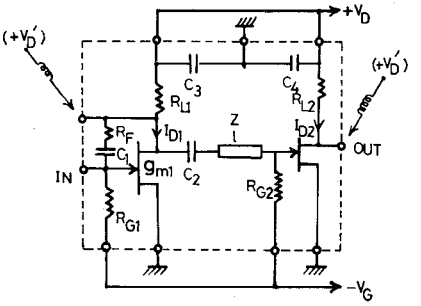

Fig. 2. Equivalent circuit for the amplifier.

I. Introduction

To realize low-noise, broad-band amplification, GaAs monolithic amplifiers having resistive loads, which are formed by GaAs active layers, have been developed [1]–[6]. To apply the amplifiers to real systems, such as mobile radio systems, temperature characteristics for the amplifier are very important.

This paper reports the results of an investigation on temperature characteristics for the amplifier having resistive loads. It is demonstrated that gain versus temperature characteristics for the amplifier are self-compensated and that the bandwidth for the amplifier becomes narrow when ambient temperature increases.

II. Theoretical Prediction

Figs. 1 and 2 show a chip photograph for the GaAs monolithic broad-band amplifier [2] and its equivalent circuit. The amplifier was fabricated on a Cr-doped semi-insulating LEC GaAs substrate. To fabricate FET's and resistors uniformly, an ion implantation technique was used. FET active (n) layers were formed by $^{30}Si^+$ ion implantation to the substrate in selected areas with energy $E = 70$ keV and dose $D = 3 \times 10^{12}$ cm^{-2}. Resistive (n^+) layers were formed by a double ion implantation. Conditions for the ion implantation are $E = 130$ keV, $D = 3 \times 10^{13}$ cm^{-2} and $E = 60$ keV, $D = 1.5 \times 10^{13}$ cm^{-2}. Dopant for the n^+ layers is $^{30}Si^+$. After the ion implantations, the substrate was coated with a CVD-SiO_2 film and annealed at 800°C (20 min) in an H_2 ambient.

To estimate the gain versus temperature characteristic for the amplifier, voltage gain $Av(T)$ for the first-stage-FET circuit in